



Research Article

Low-Frequency Impedance Spectroscopy of Wood

Tina Martin¹, Sven Nordsiek² and Andreas Weller³

¹Federal Institute for Materials Research and Testing (BAM) Berlin, Germany
and Federal Institute for Geosciences and Natural Resources (BGR) Berlin, Germany

²Technische Universität Braunschweig, Institute of Geophysics and extraterrestrial Physics,
Braunschweig, Germany

³Clausthal University of Technology, Institute of Geophysics Clausthal-Zellerfeld, Germany

Correspondence should be addressed to: Tina Martin; Tina.Martin@bgr.de

Received date: 2 June 2014; Accepted date: 22 September 2014; Published date: 19 October 2015

Academic Editor: C. Vasile

Copyright © 2015. Tina Martin, Sven Nordsiek and Andreas Weller. Distributed under Creative Commons CC-BY 4.0

Abstract

The method of low-frequency impedance spectroscopy has been successfully applied in Earth sciences to characterize soils and rocks. The method uses the diagnosing power of complex electrical resistivity in a frequency range between 1 mHz and 1 kHz. In our study, the potential of this method has been explored for the investigation of wood. We observed remarkable differences in the resulting spectra of complex resistivity for different European and tropical tree species. The data processing of the acquired low-frequency impedance spectra yields integrating parameters. The comparison of the integrating parameters with the mean pore diameter that has been separately determined for the tropical tree species indicates clear correlations. An additional investigation has revealed remarkable difference in the complex resistivity spectra between oil bearing and non-oil bearing sandal wood. This result and the relations between electrical parameters and structural parameters of wood indicate the prospective potential of low-frequency impedance spectroscopy.

Keywords: low-frequency impedance spectroscopy, spectral induced polarization, non-destructive testing, sandal wood

Introduction

The method and the instrumentation of low-frequency impedance spectroscopy have been developed as a geophysical tool for the application in Earth science. It is an electrical method that operates with galvanic coupling to the target object. It explores the electrical

properties as a function of the applied frequency. The frequency dependence of the electrical resistivity or conductivity has proved to be a valuable diagnostic parameter of soils, rocks. (e.g. Olhoeft, 1985; Börner et al., 1996; Kemna et al., 2004, Weller et al., 2010, 2013), and ores (Pelton et al., 1978; Kretschmar, 2001). Polarization effects in the

material have been identified to be the origin of the frequency dependence of electrical properties. Therefore, the method is usually referred to as Spectral Induced Polarization (SIP) in geophysics.

Considering the successful application in Earth sciences, first experiments have been made to adapt this method to wood and living trees. A variety of publications has shown that conventional electrical methods that ignore the frequency dependence are suitable for different tasks in forestry. Electrical tomographic methods can be used for the investigation of trunks, standing trees and root zones (e.g. Hanskötter, 2003; Nicolotti et al., 2003; Hagrey, 2006, 2007; Guyot et al., 2013).

The classical electrical resistivity methods have been extended considering the frequency dependence and the complex nature of electrical resistivity. The data acquisition, which is restricted to a resistivity amplitude at a single frequency for the conventional electrical methods, is extended to a measurement of impedance as a function of frequency. The electrical impedance provides both amplitude of resistance and phase shift between the current and voltage signal. The increasing amount of data that is collected has to be transferred into more information on the investigated object. Electrical impedance spectroscopy has already been successfully applied for the investigation of the physical properties of wood (Tiitta et al., 2003; Tiitta, 2006), in archaeological prospection (Schleifer et al., 2002; Weller et al., 2006, Weller and Bauerochse, 2013), the non-destructive testing of wood and trees (Martin, 2012; Martin and Günther, 2013), and for the detection of tree roots (Zanetti et al., 2011).

We present the method and instrumentation of low-frequency impedance spectroscopy and show results of recent research concerning the investigation of wood.

Low-Frequency Impedance Spectroscopy

Theory

Low-frequency impedance spectroscopy can be regarded as an extension of the conventional geoelectrical method that is characterized by a single frequency measurement. The impedance as a complex quantity that may be described by amplitude and phase is measured as a function of frequency. Using a configuration factor (dependent on the geometry of the arrangement of current and potential electrodes) the amplitude of the impedance measurement is transferred into resistivity. The phase angle results from the phase lag between current and voltage signal. The complex resistivity ρ^* is typically measured in a frequency range between 1 mHz and 1 kHz. The amplitude of resistivity $|\rho|$ is measured in Ωm and the phase ϕ is usually specified in mrad. The resulting spectra of resistivity amplitude and phase are the basis for further interpretation. A quantitative evaluation of the measured spectra can be performed by the fitting of empirical models. A common group of models is based on the Debye model (e.g. Pelton, 1978), which describes the polarization effect as a relaxation process with a time constant τ and a chargeability m . Additionally, the direct current (DC) resistivity ρ_0 is determined. The Debye decomposition approach (Nordsiek and Weller, 2008), which we use in this study, considers the complex resistivity spectra as a superposition of many relaxation processes. The amplitude and the phase spectra are transferred into a distribution of individual chargeability and relaxation time. The total chargeability m_t results from the sum of all individual chargeability values and the mean relaxation time τ_m is the weighted mean of the logarithmic relaxation times.

Experimental setup

Material and Sample Preparation

Cylindrical (20 mm in diameter and 35 to 70 mm in length, dimension error +/- 0.5 mm) or rectangular block shaped (20 mm in edge length and 70 mm in length,

dimension error +/- 0.5 mm) wood samples were cut for the investigations in laboratory. For the European tree species and the sandal wood, the samples were directly cut and measured within three days after felling to keep the original wood moisture. The samples from the tropical wood were cut from seasoned (stored) wood and wetted in tap water before measurements. To investigate the anisotropy of wood, samples

in all orientations (axial, radial and tangential) were cut and measured. We confine to the samples in axial direction in this paper.

The pore diameter distribution was determined using a mercury-porosity measuring system for the tropical wood samples.

Table 1: Parameters of the investigated wood samples

species	status		number of samples	sample shape		orientation	saturated	
	h-healthy i-infected	f-fresh s-storage		c-cylindrical b-block	a-axial, r-radial t-tangential		y-yes n-no	
European								
beech	h	f	>50	b, c	a, r	n		
oak	h	f	~ 300	b, c	a, r, t	n		
lime	h	f	~ 300	b	a	n		
poplar	h	f	12	b, c	a, r	n		
tropical								
amaranth	h	s	2	b	a	y		
ebony	h	s	10	b	a	y		
mahogany	h	s	7	b, c	a	y		
rosewood	h	s	2	b	a	y		
zebrano	h	s	4	b	a	y		
african	h	s	9	b	a	y		
blackwood								
sandal	h	f	24	b	a	n		
sandal	i	f	8	b	a	n		

Measurement Equipment

Two different impedance measurement systems were used for the laboratory investigations. The first geophysical system SIP 256C (Radic, 2008) measures the current with the remote unit RRU0 and the voltage difference across the sample with the remote unit RRU2. The second equipment is the high accuracy measurement system SIP-ZEL described in Zimmermann et al. (2008). The samples were placed into a four-electrode sample holder figure 1. An alternating

current is injected in the current electrodes C_1 , C_2 . The current flows through a coupling agent (tap water or an agar-agar solution) and the samples. The voltage difference is measured across the wood sample at the potential electrodes P_1 and P_2 . Every sample was measured several times in a frequency range between 1 mHz and 1 kHz resp. 45 kHz. To avoid temperature effects, the sample holders were placed in a conditioning cabinet ensuring a constant temperature of 20°C during the measurements.

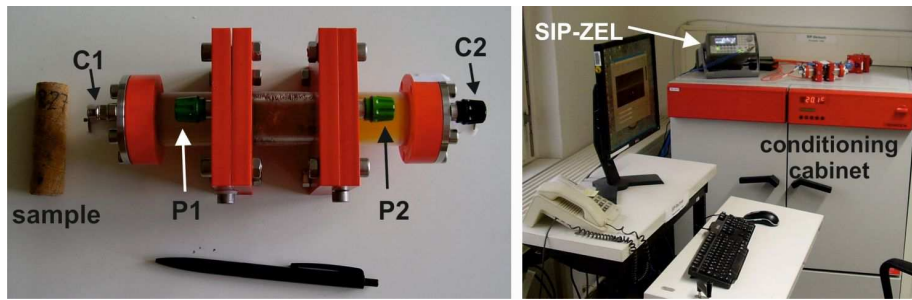


Figure 1: Equipment of the laboratory measurement. Left: Four-point-electrode sample holder with wood sample. C₁, C₂ - current electrodes, P₁, P₂ - potential electrodes. Right: System SIP-ZEL on top of the conditioning cabinet.

Results

European Tree Species

In previously published papers (Martin, 2012; Martin and Günther, 2013), it could be shown that the low-frequency impedance spectroscopy can be successfully applied on wood and standing trees. Our study is focussed on oak wood, but also other tree species were investigated. The results are shown in Figure 2. Clear differences between the four investigated European species (oak (quercus), beech (fagus), lime (tilia) and poplar (populus)) can be seen in the spectra of resistivity amplitude. Poplar wood is

characterized by the lowest resistivity amplitude ($\sim 10 \Omega\text{m}$) followed by lime wood. Oak and beech wood indicate high resistivity amplitude ($\sim 200 \Omega\text{m}$) but a different behaviour of the phase spectra. While beech wood shows a phase maximum of around 20 mrad for a frequency of 0.8 Hz, oak is characterized by a higher phase maximum (~ 25 mrad) for a much lower frequency (0.01 Hz). Poplar wood indicates the highest phase maximum with almost 40 mrad at a phase peak frequency of ~ 0.05 Hz. Lime and beech wood show a similar behavior in both amplitude and phase spectra.

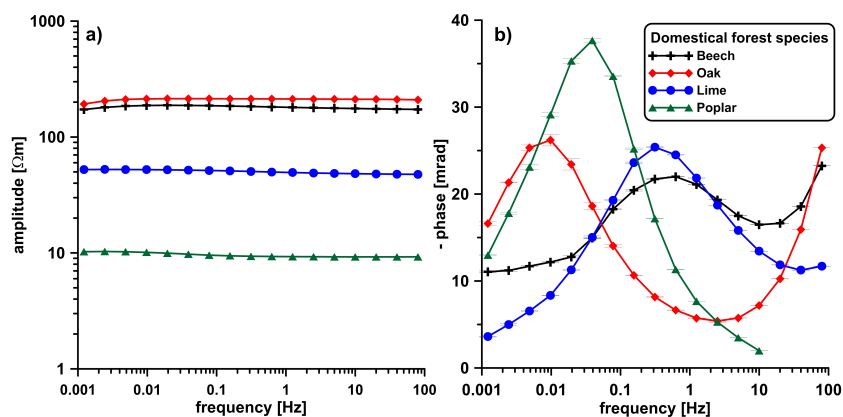


Figure 2: Amplitude (a) and phase (b) spectra of electrical resistivity from measurements at European tree species oak (quercus), beech (fagus), lime (tilia) and poplar (populus). Clear differences between the species can be seen. The error bars indicated for the phase are lower than 0.7 mrad.

Tropical Wood

Due to the different climate conditions, the structure of tropical wood differs from European tree species. As a result, the signature of the complex resistivity changes. Big differences can be seen within the tropical wood species (Figure 3). African Blackwood (*Dalbergia melanoxylon*) shows the highest resistivity amplitude but the lowest phase effect. In contrast to amaranth (*Amaranthus*) wood that shows medium resistivity amplitude ($\sim 100\Omega\text{m}$) but very high phase values (up to 140 mrad) for very low frequencies ($< 0.001\text{Hz}$). Ebony wood (*Diospyros*) and mahogany wood (*Swietenia*) are characterized by high phases (~ 60 mrad resp. > 40 mrad) at very low frequencies.

The spectra of the measurements were

analyzed by the Debye decomposition. The mean pore diameter D_m was determined by mercury injection porosimetry (after Klobes et al., 2006). In Figure 4, the mean pore diameter D_m for each tree species is plotted versus the mean relaxation time τ_m (left), versus the normalized chargeability m_t (middle) and the DC resistivity ρ_0 (right). We observe clear trends between the mean pore diameter of the tropical wood species and the integrating parameters of the Debye decomposition. The mean relaxation time and the normalized chargeability increase with increasing mean pore diameter but the DC resistivity decreases. The strongest correlation is observed for the relation between the normalized chargeability and the mean pore diameter with a coefficient of determination of $R^2 = 0.56$.

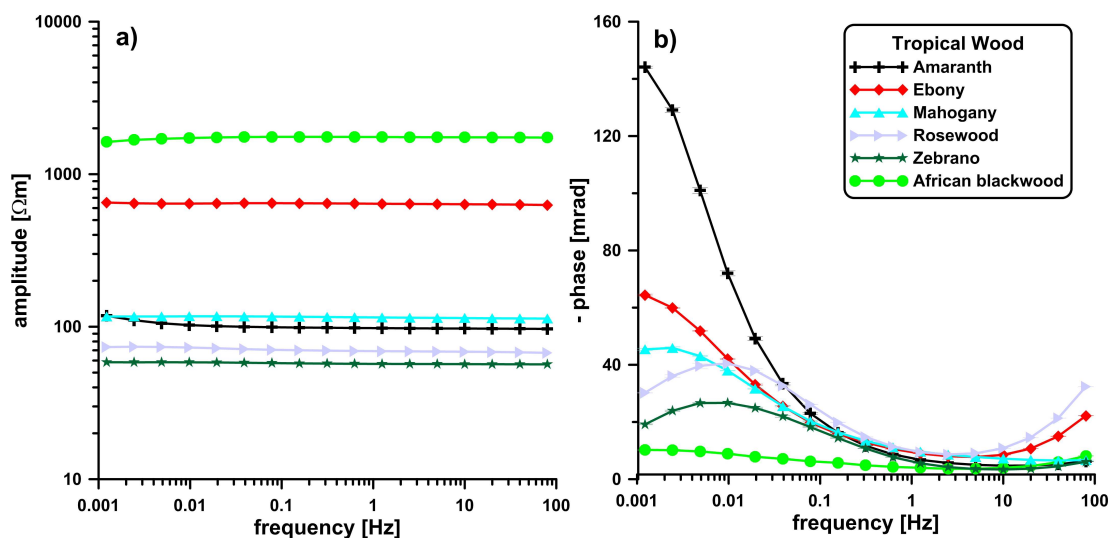


Figure 3: Amplitude (a) and phase (b) spectra of electrical resistivity measured at tropical wood samples. The error bars indicated for the phase are lower than 1.1 mrad

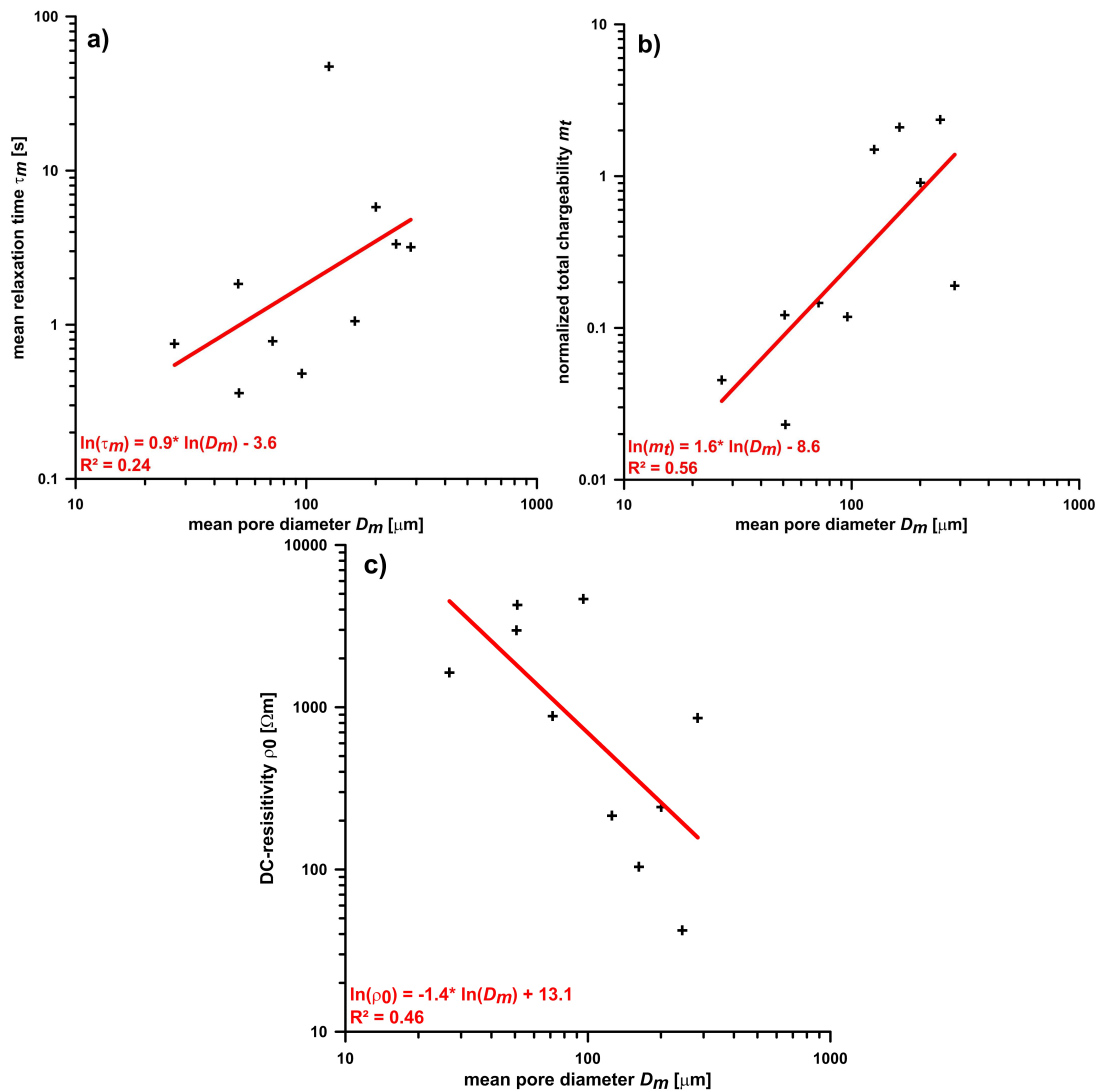


Figure 4: Comparison of mean pore diameter D_m with Debye parameters: a) mean relaxation time τ_m - coefficient of determination $R^2= 0.24$, b) normalized chargeability m_t ($R^2= 0.56$) and c) DC resistivity ρ_0 ($R^2= 0.46$)

Sandal Wood (*Santalum Album*)

A further experiment was performed on samples of sandal wood (*Santalum album*) in a different state. Adult sandal wood causes often an accumulation of oils in the heartwood. Figure 5 displays the amplitude and phase spectra of electrical resistivity of both healthy samples and oil-bearing samples. The differences in the resistivity

amplitude between healthy and oil-bearing samples are rather weak. A remarkable differentiation is observed in the phase spectra at frequencies below $f = 0.5$ Hz. The healthy sandal wood is only weakly polarizable (phase ~ 10 mrad) whereas the infected parts indicate maximum phase values between 30 mrad and 42 mrad at $f \approx 0.02$ Hz.

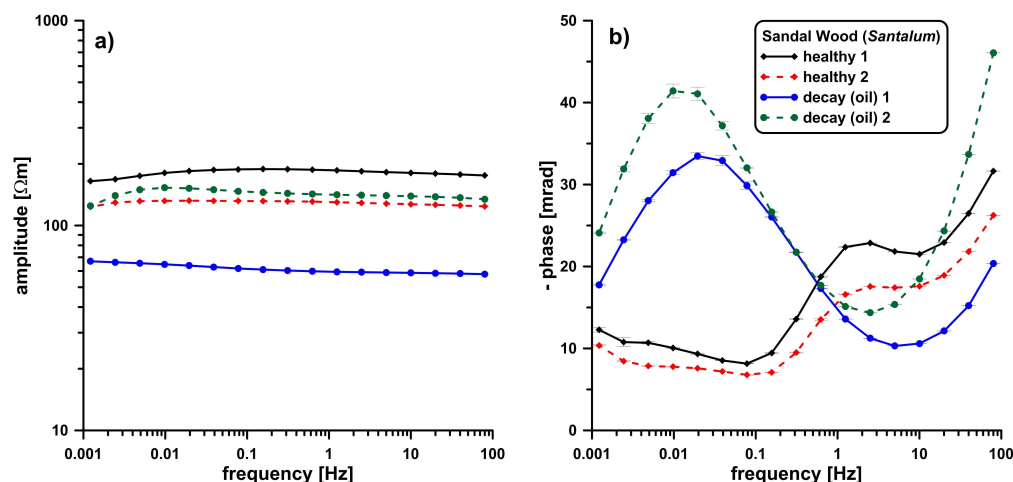


Figure 5: Amplitude (a) and phase (b) spectra of electrical resistivity measured for healthy and infected (oil saturated) sandal wood samples. The error bars indicated for the phase are lower than 0.6 mrad

Discussion

The results from the European tree species show a remarkable variation between the different species. In our study, poplar wood was identified to be both the most conductive (low resistivity amplitude) and the most polarizable (high phase shift) material. The high conductivity may be caused by a stronger ion concentration of the intercellular fluids. The cell structure and the wood design cause a membrane effect that is related to polarization. Oak wood and beech wood show similar values for the resistivity amplitude but the phase signature is different. The maximum phase lag for oak wood is located at much lower frequencies (~ 0.01 Hz) than for beech wood (~ 1 Hz). The shift of the phase peak indicates differences in geometry and structure of the wooden cells.

Regarding African Blackwood and amaranth wood, strong differences can be observed for tropical wood species, too. African Blackwood wood shows the highest resistivity amplitude and almost no phase effect (constant phase). The highest phase lag is observed for amaranth wood with remarkable > 140 mrad at very low frequencies (< 0.001 Hz) but the resistivity

amplitude remains at low level.

The frequency of the phase peak is identified to be the most significant difference between European species and tropical wood species. We observed the phase peak for almost all tropical wood species definitely at lower frequencies in comparison with the phase peak of the European wood species. The reason for that seems to be the visible different internal wood structure.

Despite all differences between the varying tropical wood species, the results from the Debye decomposition show a kind of power-law-relations between mean pore diameter and all integration parameters of the Debye decomposition. We found that the relaxation time (outlier: amaranth) and the normalized chargeability increase with the mean pore diameter. DC resistivity decreases with the mean pore diameter. Due to the observed correlation between mean pore diameter and the integrating parameters of the Debye decomposition, it might be possible to derive information on the pore diameter respectively information about the condition of the wood cell directly from the low-frequency impedance spectra.

Differences between oil-bearing and non-oil-bearing sandal wood are observed in the

phase spectra. The indication of valuable oil-bearing wood is identified as a potential field of application for the low-frequency impedance spectroscopy. It should be noted that the complex resistivity spectra of fungi-infected wood samples show much lower phases for the infected wood compared to the healthy wood samples (Martin, 2012). The reduction in phase shift was attributed to the destruction of the polarizable wood cell structure. The sandal wood indicates an inverse effect. An increase of the phase shift is observed for the infected wood samples. We assumed that the interface between oil and wood might cause a stronger polarization.

Summary and Conclusions

Low-frequency spectroscopy shows a considerable potential for the investigation of trees and wood. We identified the following fields of application:

- Non-destructive testing of trees e.g. for the stability of trees in public areas. Differentiation between healthy and infected wood within standing trees.
- Information about the integrated pore volume or the condition of the wood cells of living trees.
- Determination of oil-bearing wood for sandal wood trees. Information about maturation and therefore a diagnosis to the best time for felling.
- Characterization of different tropical wood species.

Despite all investigations carried out so far, a lot of research has still to be done. The relationship between the low-frequency complex resistivity signature and the internal wood structure has to be analyzed in more detail. A comparison between the results of low-frequency impedance spectroscopy and other structure resolving methods like microscope, scanning electron microscope (SEM), chemical analysis, and acoustic methods, are indispensable. The low-frequency impedance spectroscopy offers the potential to be a promising additional tool for the investigation of wood and trees.

Acknowledgement

All investigations were made at the Federal Institute for Materials Research and Testing (BAM). Parts of the (European wood) data were collected within the ProInno project *Zerstörungsfreie Baumuntersuchungstechnologien* raised by the Federal Ministry of Economics and Technology. The sandal wood was provided by the company *argus electronic gmbh*. The analysis of some data and the compilation of the paper were made at the Federal Institute for Geoscience and Natural Resources (BGR), at Braunschweig University of Technology, and at Clausthal University of Technology.

References

1. Börner, F., Schopper, J. and Weller, A. (1996) "Evaluation of transport and storage properties in the soil and groundwater zone from induced polarization measurements," *Geophysical Prospecting*, 44, 583 – 601.
2. Guyot, A., Ostergaard, K. T., Lenkopane, M., Fan, J. and Lockington, D. A. (2013) "Using electrical resistivity tomography to differentiate sapwood from heartwood: application to conifers," *Tree Physiology*, 33, 187 pp.
3. Hagrey, S. (2006) "Electrical resistivity imaging of tree trunks," *Near Surface Geophysics*, 4, 177 – 185.
4. ----- (2007) "Geophysical imaging of root-zone, trunk and moisture heterogeneity," *Journal of Experimental Botany*, 58, 839 – 854.
5. Hanskötter, B. (2003) „Diagnose fakultativer Farbkerne an stehender Rotbuche (*Fagus sylvatica* L.) mittels elektrischer Widerstandstomographie," *PhD thesis*, Georg-Augst-Universität Göttingen, Germany, Cuvillier Verlag Göttingen.
6. Kemna, A., Binley, A. and Slater, L. (2004) "Crosshole IP imaging for engineering and environmental applications," *Geophysics*, 69, 97 – 107.

7. Klobes, P., Meyer, K. and Munro, R.G. (2006) "Porosity and Specific Surface Area Measurements for Solid Materials", Special Publication 960-17, NIST practice guide.
8. Kretschmar, D. (2001) „Untersuchung zur Inversion von spektralen IP-Daten unter Berücksichtigung elektromagnetischer Kabelkopplungseffekte," PhD thesis, Technische Universität Berlin, Germany.
9. Martin, T. (2012) "Complex resistivity measurements on oak," *European Journal of Wood and Wood Products*, 70, 45–53.
10. Martin, T. and Günther, T. (2013) "Complex Resistivity Tomography (CRT) for fungus detection on standing oak trees," *European Journal of Forest Research* 132 (5), 1-12.
11. Nicolotti, G., Socco, L., Martinis, R., Godio, A. and Sambuelli, L. (2003) "Application and comparison of three tomographic techniques for detection of decay in trees," *Journal of Aboriculture*, 29, 66–78.
12. Nordsiek, S. and Weller, A. (2008) "A new approach to fitting induced-polarization spectra," *Geophysics*, 73, F235 – F245.
13. Olhoeft, G. (1985) "Low-frequency electrical properties," *Geophysics*, 50, 2492 – 2503.
14. Pelton, W., Ward, S., Hallof, P., Sill, W. and Nelson, P. (1978) "Mineral discrimination and removal of inductive coupling with multifrequency IP," *Geophysics*, 43, 588 – 609.
15. Radic, T. (2008) „Instrumentelle und auswertemethodische Arbeiten zur Wechselstromgeoelektrik," PhD thesis, Technische Universität Berlin, Germany.
16. Schleifer, N., Weller, A., Schneider, S. and Junge, A. (2002) "Investigation of a Bronze Age plankway by spectral induced polarization," *Archaeological Prospection*, 9, 243–253.
17. Tiitta, M. (2006) "Non-destructive methods for characterisation of wood material," *PhD thesis*, University of Kuopio, ISBN 951-27-0680-6.
18. Tiitta, M., Kainulainen, P., Harju, A., Venäläinen, M., Manninen, A.-M., Vuorinen, M. and Viitanen, H. (2003) "Comparing the effect of chemical and physical properties on complex electrical impedance of Scots pine wood," *Holzforschung*, 57, 433–439.
19. Weller, A., Nordsiek, S. and Bauerochse, A. (2006) "Spectral induced polarisation - a geophysical method for archaeological prospection in peatlands," *Journal of Wetland Archaeology*, 6, 105–125.
20. Weller, A., Slater, L., Nordsiek, S. and Ntarlagiannis, D. (2010) "On the estimation of specific surface per unit pore volume from induced polarization: A robust empirical relation fits multiple datasets," *Geophysics* 75, No. 4, WA105-WA112.
21. Weller, A. and Bauerochse, A. (2013) "Detecting organic materials in waterlogged sediments" – in: Menotti, F.; O'Sullivan, A. (Editors) *The Oxford Handbook of Wetland Archaeology*, Oxford University Press, p. 421-432.
22. Weller, A., Slater, L. and Nordsiek, S. (2013) "On the relationship between induced polarization and surface conductivity: Implications for petrophysical interpretation of electrical measurements," *Geophysics* 78, No. 5, D315-D325.
23. Zanetti, C., Weller, A., Vennetier, M. and Meriaux, P. (2011) "Detection of buried tree root samples by using geoelectric measurements: a laboratory experiment," *Plant and Soil*, 339, 273–283.
24. Zimmermann, E., Kemna, A., Berwix, J., Glaas, W., Muench, H.M. and Huisman, J. (2008) "A high-accuracy impedance spectrometer for measuring sediments with low polarizability," *Measurement Science and Technology*, 19, 105603 (9pp).